

Contributions of biological tumor parameters to the incorporation rate of L-[methyl-¹¹C] methionine into astrocytomas and oligodendrogliomas

Takeko Nojiri · Tadashi Nariai · Masaru Aoyagi ·
Michio Senda · Kenji Ishii · Kiichi Ishiwata ·
Kikuo Ohno

Received: 20 September 2008 / Accepted: 9 December 2008 / Published online: 20 December 2008
© The Author(s) 2008. This article is published with open access at Springerlink.com

Abstract We compared the tumor uptake of ¹¹C-methionine (MET) with positron emission tomography (PET) with the results of a pathological analysis to examine the proliferative potential and microvessel density measured with immunostaining for MIB-1 and factor VIII, respectively, from 33 patients with glioma. The MET uptake in oligodendrogliomas was significantly greater than that in grade 2 astrocytomas and comparable to those in grade 3 and 4 astrocytomas. The MIB-1 index of oligodendroglioma meanwhile was comparable to that of grade 2 astrocytoma. The microvessel area in oligodendroglioma was significantly greater than that in grade 2 astrocytomas and comparable to those in grade 3 and 4 astrocytomas. According to a multivariate statistical analysis, MET uptake ratio was closely correlated with the MIB-1 index among astrocytomas. An increase in the microvessel area in the oligodendrogliomas contributed to the higher MET uptake among the tumors with a low-proliferative index. This information is important for interpreting the results of MET-PET studies for clinical use.

Keywords Positron emission tomography · ¹¹C-methionine · Proliferative index · Microvessel density · Oligodendroglioma · Astrocytoma

Introduction

Morphological imaging using magnetic resonance imaging (MRI) with gadolinium (Gd) contrast enhancement is the most widely accepted method for diagnosis in the treatment of gliomas. The technique has the drawback, however, of frequent false negatives in tumor regions without blood–brain barrier (BBB) breakdown. The contrast enhancement reflects regions of BBB breakdown, whereas glioma cells usually infiltrate the brain structure without BBB breakdown [1–5]. Positron emission tomography (PET) with appropriate metabolic tracers plays an important role in characterizing and delineating gliomas in infiltrative zones of this type.

The PET examination of ¹¹C-methionine (MET) uptake, the technique generally considered to provide the most reliable images for evaluating glioma, has been reported to delineate gliomas more accurately than MRI [6–9]. ¹¹C-methionine readily crosses the intact BBB and is incorporated into the active tumor cells via the neutral amino acid transporter system [10, 11]. As a consequence, MET-PET can delineate the infiltration of malignant glioma cells beyond the area with gadolinium enhancement in MRI [12]. MET-PET can thus be expected to serve well for the accurate planning of radical resections of gliomas [13]. The degree of ¹¹C-methionine uptake expressed as a ratio to control brain has also been found to be an important factor in predicting the survival periods of patients with gliomas [6, 14, 15].

T. Nojiri · T. Nariai (✉) · M. Aoyagi · K. Ohno
Department of Neurosurgery, Tokyo Medical and Dental
University, 1-5-45, Yushima, Bunkyo-ku, Tokyo, Japan
e-mail: nariai.nsr@tmd.ac.jp

M. Senda
Department of Image-Based Medicine, Institute of Biomedical
Research and Innovation, Kobe, Japan

K. Ishii · K. Ishiwata
Positron Medical Center, Tokyo Metropolitan Institute of
Gerontology, Tokyo, Japan

As these previous reports indicate, MET-PET imaging certainly serves as a useful clinical tool in the course of glioma treatment. There is some uncertainty, however, in the mechanism of methionine uptake into the tumor. In one biochemical analysis, ^{11}C -methionine uptake was reported to reflect both protein synthesis in tumor cells and amino acid transport in tumor endothelial cells [16]. Several reports have suggested that ^{11}C -methionine uptake measured with PET reflects the proliferative index of gliomas [17, 18] and microvessel density of tumor tissue, putative markers of protein synthesis and amino acid transport through microvessels, respectively [19].

We speculated that an understanding of the correlations of MET uptake, proliferative index, and microvessel density with various types of glioma may help to clarify the mechanism of MET uptake into glioma. In the present report we retrospectively analyzed our preoperative ^{11}C -methionine PET data to examine whether ^{11}C -methionine uptake correlates with histopathological analyses of the proliferation index and microvessel density in gliomas, mainly focusing on the difference between astrocytomas and oligodendrogliomas.

Materials and methods

Patients

Tumor specimens were obtained from 33 patients with supratentorial gliomas who underwent surgery and preoperative ^{11}C -methionine PET studies from 1992 to 2001 in our institution. The subjects included 14 females and 19 males with a mean patient age of 45.5 ± 12.9 (standard deviation, SD) years. Immediately after surgical resection, the tumor samples were fixed in 4% paraformaldehyde in 0.1 M phosphate buffer for 24 h and embedded in paraffin. The tumor samples were stained with hematoxylin and eosin, then classified according to the malignancy criteria of the World Health Organization (WHO).

PET scans and data analysis

PET measurements were carried out by measuring the equilibrated radioactivity 20 min after i.v. MET injection (250–500 MBq) using a PET scanner (Headtome IV or V, Shimadzu, Kyoto, Japan). The transmission data were acquired for each patient with a rotating germanium-68 rod source for attenuation correction. The regional uptake of MET was expressed as a standardized uptake value (SUV) (tissue activity/ml)/(injected radioisotope activity/body weight (g)) and the uptake into the tumor was expressed as the ratio of SUV to the contralateral normal brain (T/N

ratio). To determine the SUV of the tumor, the regions of interest (ROIs) were manually placed over the tumor area on a maximum of four axial images by one of the authors Nariai. When the lesion was difficult to detect on the PET image, the PET data were registered with the patient's MRI data for determination on MRI. The image fusion was performed using an automated image analysis program [20] in combination with Dr. View v 5.3 image analysis software (Asahi Kasei Information System, Co. Ltd., Tokyo, Japan) on a personal computer.

Cell proliferative index

The cell proliferation rate was measured using a monoclonal antibody (MIB-1) against nuclear antigen Ki-67 (Immunotech S. A., Marseille Cedex). The sections were pretreated in an autoclave to enhance immunoreactivities, according to the method of Shin et al. [21, 22] with some modification. After deparaffinization in xylene and rehydration in ethanol, 4 mm sections were autoclaved at 121°C for 15 min in a stainless-steel vessel filled with 10 mM citrate buffer, pH 6.0, to completely immerse the sections. Immunohistochemical detection was carried out using a labeled streptavidin–biotin method with a LSAB kit (DAKO, Kyoto, Japan). The sections were incubated with the primary antibody for 60 min, reacted in sequence with biotinylated link antibody (goat antibody to mouse and rabbit immunoglobulins) followed by peroxidase-labeled streptavidin, developed with diaminobenzidine, and counterstained with hematoxylin. Cell proliferation was assessed by screening the slides at low magnification and finding high proliferative areas by one of another author Nojiri without knowing the PET data. Tumor cells with nuclear staining were regarded as positive for MIB-1. The proliferative index (i.e., positive cells per all tumor cells) was then calculated as a percentage by counting more than 500 tumor cell nuclei from three microscopic fields at 400 \times magnification (the mean of three values was used).

Tumor microvessel density

A rabbit polyclonal antibody against human factor VIII-related antigen (DAKO, Kyoto, Japan) was used to stain capillary endothelium. The tumor microvessel density was represented by the tumor microvessel count and tumor microvessel area. The tumor microvessel count was determined by counting the numbers of tumor capillary vessels per field (0.245 mm²) in three highly vascularized areas at 200 \times magnifications (the mean of the three values was used). The tumor microvessel area was determined by calculating the area of tumor capillary vessels per field (0.173 mm²) and quantified by densitometric scanning with

an NIH image program for Macintosh in three highly vascularized areas at 200 \times magnification. The percentage of the area inside the microvessel in the digitized field (0.173 mm²) was calculated as the mean of three digitized fields. The three highly vascularized areas were determined by one of another author Nojiri without knowing the PET data.

Statistical analysis

All values were expressed as means \pm standard deviation (SD). The differences in the mean values of measured parameters among various grades of gliomas were compared between oligodendrogliomas and three grades of astrocytomas by one-way analysis of variance and Dunnett's post hoc test. Correlation among the ¹¹C-methionine uptake ratio, MIB-1 index, and the area of tumor microvessels per field was analyzed using multivariate analysis of variance and multifactorial regression analysis. Statistically significant difference was determined as $P < 0.05$.

Results

Proliferative potentials and methionine uptake on PET in oligodendrogliomas and astrocytomas

The glial tumors were histologically diagnosed by hematoxylin and eosin staining and classified according to the malignancy criteria of the World Health Organization (WHO). Twenty-six cases were diagnosed as astrocytomas and seven cases were diagnosed as oligodendrogliomas. Thirteen cases of astrocytomas were classified as grade 2, seven were classified as grade 3, and six were classified as grade 4, according to the WHO criteria. All seven oligodendrogliomas were classified as grade 2.

The methionine uptake in the PET study on astrocytomas increased for higher tumor grades. That in grade 2 oligodendrogliomas was significantly higher than that in grade 2 astrocytomas, but not significantly different from those in grade 3 and 4 astrocytomas (Fig. 1a).

The proliferative activity calculated by MIB-1 staining indices was quite consistent with the tumor uptake ratio of methionine in the PET study on astrocytomas. The MIB-1 indices of grade 2 oligodendrogliomas were low, were significantly different from those of grade 2 astrocytomas, and were significantly lower than those of grade 3 and 4 astrocytomas (Fig. 1b).

Representative ¹¹C-methionine PET images and photomicrographs of MIB-1 immunostaining in gliomas are displayed side by side in Fig. 2. The ¹¹C-methionine uptake ratio and proliferative index both increased stepwise with

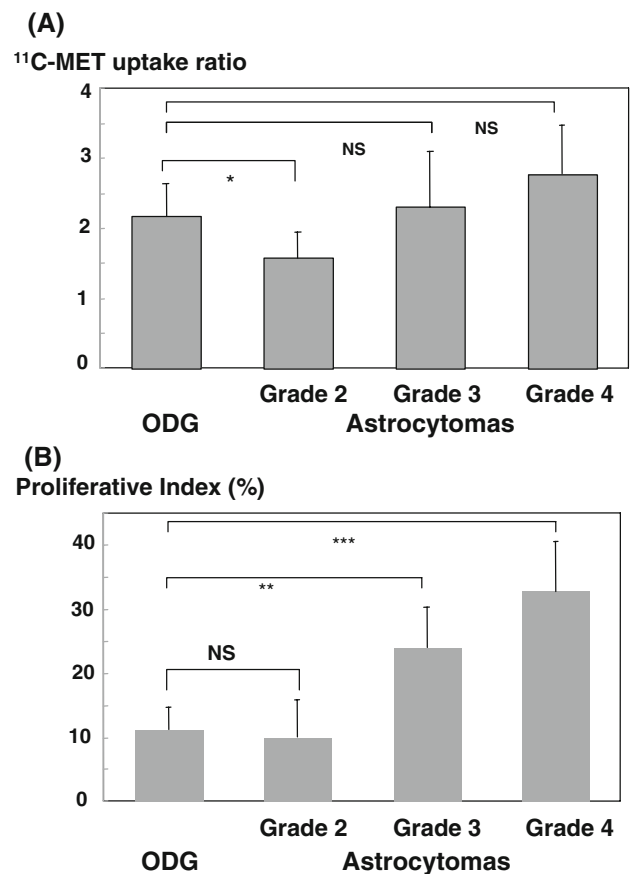


Fig. 1 a Bar graphs to compare the ¹¹C-methionine uptake ratio in gliomas. ODG, grade 2 oligodendrogliomas; Grade2, grade 2 astrocytomas; Grade3, grade 3 astrocytomas; Grade4, grade 4 astrocytomas. The ¹¹C-methionine uptake ratio in ODG was significantly higher than that in Grade 2 but not significantly different from those in grade 3 and 4 astrocytomas. In astrocytomas, the methionine uptake ratio increases stepwise with increasing tumor grades. * $P < 0.05$. NS: not significantly different. b Bar graphs to compare the proliferative index of gliomas. ODG, grade 2 oligodendrogliomas; Grade2, grade 2 astrocytomas; Grade3, grade 3 astrocytomas; Grade4, grade 4 astrocytomas. In astrocytomas, the MIB-1 indices increased stepwise with increasing tumor grades. The MIB-1 indices in ODG were significantly lower than those of grade 3 and 4 astrocytomas and were not significantly different from those of grade 2 astrocytoma. ** $P < 0.01$. *** $P < 0.001$. NS: not significantly different

increases in tumor grade, as demonstrated in Fig. 2a–c. The ¹¹C-methionine uptake ratio in the oligodendroglioma (Fig. 2d), was higher than that of the grade 2 astrocytoma (Fig. 2a) in spite of similar MIB-1 staining.

Tumor microvessel characteristics in oligodendrogliomas and astrocytomas

Figure 3 shows representative immunostaining for factor VIII-related antigen in tissue sections of grade 2, 3, 4 astrocytomas and grade 2 oligodendrogliomas. The number of tumor blood vessels appears to increase with increasing

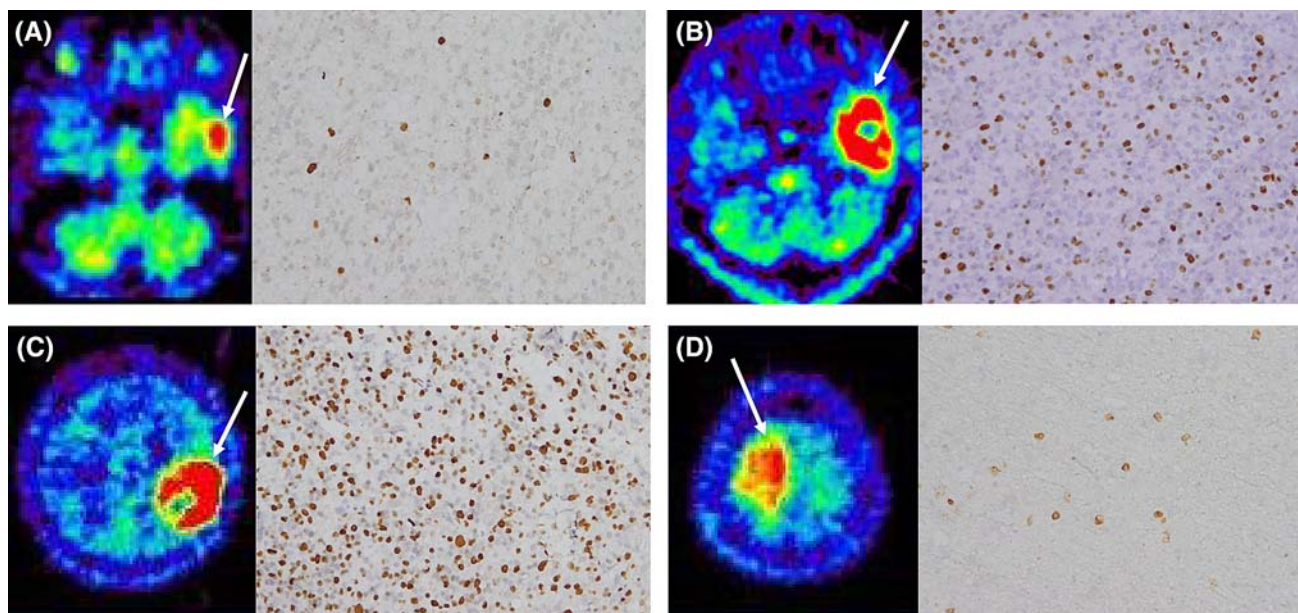
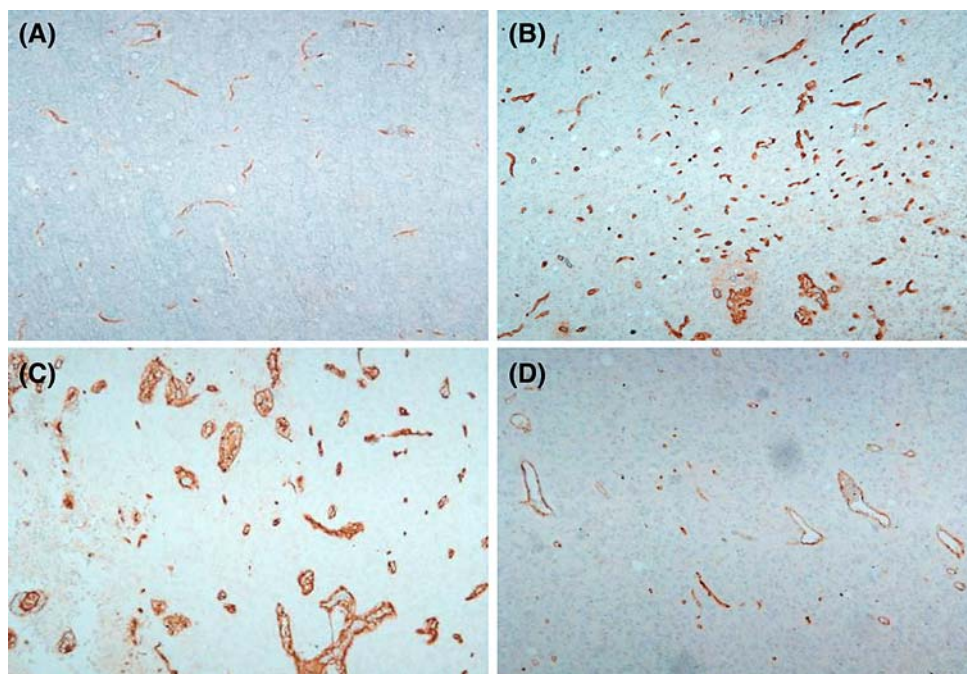


Fig. 2 ^{11}C -methionine PET images and photomicrographs of MIB-1 immunostaining in gliomas (Original magnification, $200\times$) were displayed side by side for representative cases. **a** 33-year-old female with grade 2 astrocytoma. ^{11}C -methionine PET image (left) showing mildly elevated uptake of methionine in the tumor, indicated by arrow. The ratio of methionine uptake into the tumor compared to the contralateral normal brain (T/N) was 1.4. The proliferative index measured with MIB-1 immunostaining was 11% (right). **b** 39-year-old male with grade 3 astrocytoma. ^{11}C -methionine PET image (left) showing higher uptake of methionine in the tumor (arrow) in comparison to the grade 2 tumor. The T/N of the methionine uptake

was 2.5. The proliferative index measured with MIB-1 immunostaining was 37% (right). **c** 46-year-old female patient with grade 4 astrocytoma. ^{11}C -methionine PET image (left) showing the highest methionine uptake among the images in this figure (arrow). The T/N of the methionine uptake was 4.0. The proliferative index measured with MIB-1 immunostaining was 44% (right). **d** 56-year-old female patient with grade 2 oligodendroglioma. ^{11}C -methionine PET image (left) showing higher methionine uptake than that in the grade 2 astrocytoma (arrow). The T/N of the methionine uptake was 1.95. The proliferative index measured with MIB-1 immunostaining was 14% (right)

Fig. 3 Immunostaining of factor VIII-related antigen for the staining of capillary endothelium in tissue sections of gliomas (Original magnification, $200\times$), for representative cases. **a** The grade 2 astrocytoma shows a small number of microvessels. **b** The grade 3 astrocytoma shows a greater increase in the number of microvessels than the grade 2 tumor. **c** The grade 4 astrocytoma shows a larger number of microvessels with glomeruloid body formation. **d** The grade 2 oligodendroglioma shows only a small number of microvessels, but those shown are enlarged and branching



tumor grade in the astrocytomas. The grade 4 astrocytomas, that is, the glioblastomas, typically showed endothelial hyperplasia with glomeruloid body formation (Fig. 3c). We compared the tumor blood vessel density by counting the number of capillary blood vessels per high power field in sections stained with antibodies against factor VIII-related antigens (Fig. 4a). The microvessel count in grade 2 oligodendrogliomas did not differ from that in grade 2 astrocytomas but fell significantly below those in grade 3 and 4 astrocytomas. The microvessels of oligodendroglioma, on the other hand, were morphologically distinct and apparently larger than those in the grade 2 astrocytomas (Fig. 3a, d). Noting these findings, we decided to compare

not only the number of microvessel per area of specimen, but also the area of tumor capillary blood vessels per field. The percent microvessel area per field in astrocytomas increased with increasing tumor grade. The microvessel area in the grade 2 oligodendrogliomas was significantly greater than that in grade 2 astrocytomas, but not significantly different from those in grade 3 and 4 astrocytomas. The mean value of percent microvessel area was greater in the oligodendrogliomas than in the grade 4 astrocytomas.

Multivariate statistical analysis to examine the correlations among the ^{11}C -methionine uptake ratio, proliferative index, and microvessel area in oligodendrogliomas and astrocytomas

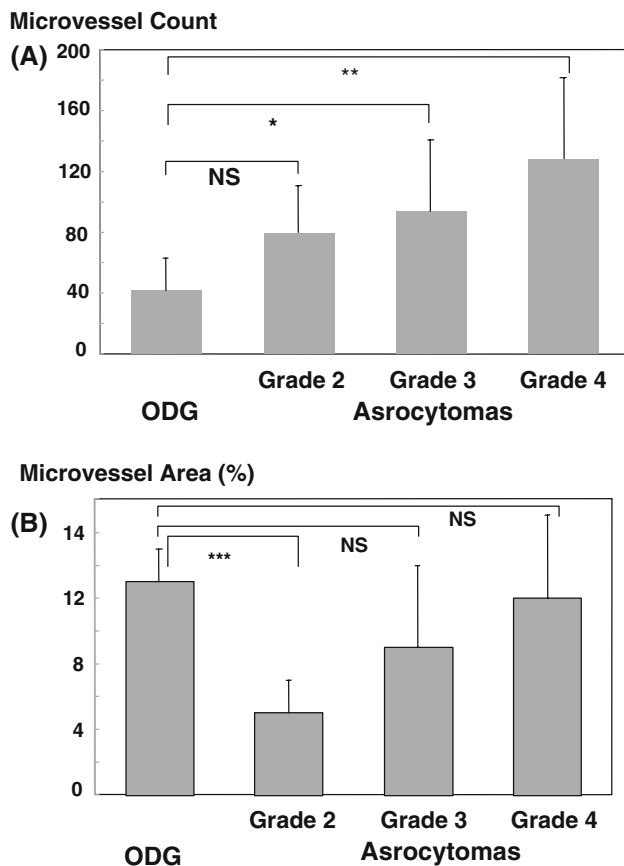


Fig. 4 **a** Bar graphs to compare tumor microvessel count in gliomas. ODG, grade 2 oligodendrogliomas; Grade2, grade 2 astrocytomas; Grade3, grade 3 astrocytomas; Grade4, grade 4 astrocytomas. In the astrocytomas, the microvessel count increased stepwise with increasing tumor grades. The microvessel count in grade 2 oligodendrogliomas did not significantly differ from that in grade 2 astrocytomas and was significantly less than those in grade 3 and 4 astrocytomas. * $P < 0.05$. ** $P < 0.01$. NS: not significantly different. **b** Tumor microvessel area in gliomas. In the astrocytomas, the differences in the microvessel area became more significant than the differences in the microvessel count. The microvessel area in the grade 2 oligodendrogliomas was significantly greater than that in the grade 2 astrocytomas ($P < 0.001$) and corresponded to that in the grade 4 astrocytomas

The three charts in Fig. 5 plot out the correlations among the ^{11}C -methionine uptake ratio, percent microvessel area per field, and proliferative index in oligodendrogliomas and astrocytomas. The oligodendrogliomas are plotted with white circles, and the 50% confidence range of normal two-factor distribution is indicated in the ellipsoid with a solid line. Astrocytomas are plotted with black dots and the 50% confidence range of normal two-factor distribution is indicated in the ellipsoid with the dotted line. Multivariate analysis indicated that the oligodendrogliomas and astrocytomas had significantly different distributions in three-dimensional space composed of these three parameters ($P < 0.0001$). The plots of the oligodendrogliomas indicate a lower proliferative index and higher microvessel area than the plots of the astrocytomas.

Figure 5 shows the pair-wise correlation coefficient for oligodendrogliomas and astrocytomas. A partial correlation coefficient, drawn by multiple regression analysis by excluding the effect of another factor, is displayed as a matrix in Table 1. All these data indicate that the methionine uptake ratio in the astrocytomas depend heavily on the proliferative index rather than the microvessel area. In the oligodendrogliomas, the methionine uptake ratio correlated with the microvessel area, but not with the proliferative index. The correlation between proliferative index and microvessel area also differed between the astrocytomas and oligodendrogliomas. A significant positive correlation was observed in the former and a negative correlation was observed in the latter.

Discussion

^{11}C -methionine PET provides important information for both the histological malignancy and tumor viability in brain gliomas. Several reports have shown that methionine uptake measured by PET is positively correlated with the proliferative activity of gliomas [17, 18, 23]. The in vitro

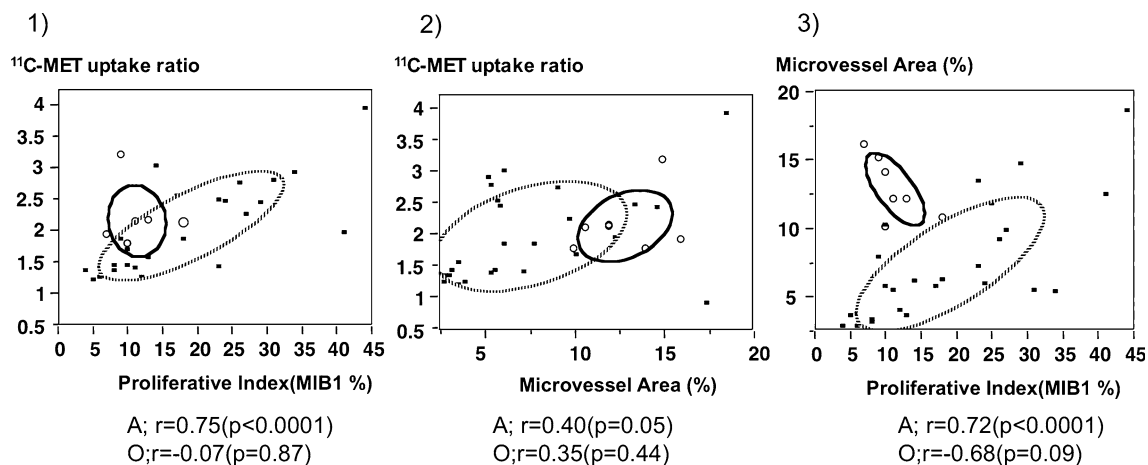


Fig. 5 Three plots to demonstrate the correlation among the ^{11}C -methionine uptake ratio, proliferative index, and microvessel area in oligodendrogliomas and astrocytomas. Plot 1 indicates the correlation between the proliferative index (%) and ^{11}C -methionine uptake ratio. Plot 2 indicates the correlation between the percent microvessel area per field and the ^{11}C -methionine uptake ratio. Plot 3 indicates the correlation between the proliferative index (%) and

microvessel area (%). Oligodendrogliomas were plotted as white circles. Astrocytomas were plotted with black dots. Ellipsoids are indicated for oligodendrogliomas (solid line) and astrocytomas (dotted line) to indicate 50% normal distribution in two dimensions. Pair-wise correlation coefficient was displayed beneath each plot for oligodendrogliomas (O) and astrocytomas (A)

Table 1 Partial correlation matrix among MET-ratio, MIB-1 index (%), and microvessel area (%) astrocytomas and oligodendrogliomas

	MET-ratio	MIB-1 index (%)	Microvessel area (%)
MET-ratio	/	0.5634*	0.1867*
MIB-1 index (%)	0.2338 ^a	/	0.4785*
Microvessel area (%)	0.4047 ^a	-0.6974 ^a	/

* Partial correlation coefficient among astrocytomas

^a Partial correlation coefficient among oligodendrogliomas

transport of [^3H -methyl]-L-methionine depends on the proliferation rate of human glioma cells [24]. The tumor cell density and proliferative activity increase in tumors of higher malignancy grade, hence the amino acid transport and protein synthesis in the tumor cells are thought to increase accordingly. Our data from the present study revealed that the ^{11}C -methionine uptake ratios in astrocytomas were positively correlated with the histological malignancy grade and the proliferative activity estimated by MIB-1 staining indices. The proliferative indices in grade 2 oligodendrogliomas were low, and similar to those in grade 2 astrocytomas. The ^{11}C -methionine uptake in grade 2 oligodendrogliomas, on the other hand, was significantly higher than that in grade 2 astrocytomas and corresponded to those in grade 3 or 4 astrocytomas. A higher methionine uptake in oligodendrogliomas on PET has been reported earlier [15, 25], and the mechanism of the dissociation between the methionine uptake and proliferative potentials has been discussed. The cellular density or absence of necrosis is unlikely to contribute to the higher uptake of methionine in grade 2 oligodendrogliomas. Rather, the high ^{11}C -methionine uptake in grade 2

oligodendrogliomas is thought to be associated with factors other than the protein synthesis of the tumor cells. Another report has suggested that the cell type strongly influences the degree to which microvessel density contributes to tumor viability. Microvessel density is an important prognostic indicator for patients with astrocytomas [26], but it has no apparent influence on the survival of patients with oligodendrogliomas [27]. According to the biochemical analyses by Ishiwata et al. [16], the in vivo uptake of radiolabeled methionine into tumors is influenced both by the rate of protein synthesis and rate of amino acid transport rate from blood into the tumor cells. Thus, we can reasonably infer that these two factors may confer different influences, depending on the tumor cell type. Our present data and literature review suggest that the methionine uptake into oligodendroglioma depends on the higher amino acid transport rate, but not on the increased rate of protein synthesis, whereas the methionine uptake into astrocytoma depends strongly on the increased rate of protein synthesis (i.e., the increased cell proliferation rate).

The amino acid transport mechanism from blood to brain or tumor has been well investigated. Methionine is

one of the large neutral amino acids. Large neutral amino acids share a single transporter that can be characterized as a Na⁺-independent system L in the luminal membrane of the BBB [10, 11]. System L transporter was originally described by Oxender and Christensen [28]. The 4F2hc surface antigen, a known marker of normal and neoplastic cell growth, has been identified as an activator of system L transporter [29]. The system is currently referred to as the “large neutral amino acid transporter 1” (LAT1). LAT1 is reported to be strongly expressed several tumor cell lines [24] and in tumor endothelial membrane [30, 31]. The physiology of amino acid transport has also been well theorized. The rate of transfer through the transporter is determined by the product of permeability and surface area of the vessels [32, 33]. Once we suppose that the transporter itself has the same molecular structure among brain and tumor microvessels and distributes evenly in the endothelial wall, we can determine the transfer rate by the surface area of the microvessels. An increased number of microvessels per tissue volume and the enlargement of individual microvessels can both lead to a higher surface area of microvessels.

Others have investigated the correlation between methionine uptake and the characteristics of brain and tumor microvessels. The accumulation of ¹¹C-methionine in the normal brain tissue and the microvessel count of non-tumoral brain are both higher in gray matter than in white matter [34, 35]. There is no difference of ¹¹C-methionine uptake between tissues with and without endothelial proliferation [36]. There have been conflicting results as to the microvessel counts in oligodendrogliomas. Some reports have suggested that, there are more microvessels in grade 2 oligodendrogliomas than in grade 2 astrocytomas [19, 36], while others have shown that the microvessel count of oligodendroglioma was similar to that of astrocytoma grade 2 [37]. Kracht et al. recently identified a strong correlation between the number of microvessels and the ¹¹C-methionine uptake in gliomas [19]. The microvessels count in our study increased together with the tumor grade in astrocytoma, whereas that in grade 2 oligodendrogliomas was significantly smaller than in grade 2 astrocytomas. Our results indicate that the higher ¹¹C-methionine uptake in grade 2 oligodendrogliomas is not caused by an increase in the microvessel count.

We previously found that, the concentrations of endostatin, an endogenous inhibitor of angiogenesis, are strongly correlated with the tumor microvessel area per field, but only weakly correlated with the number of tumor microvessels per field [38]. As each microvessel of grade 2 oligodendrogliomas appeared to be both enlarged and branching, we decided to estimate the microvessel area instead of the microvessel count. The microvessel area in oligodendrogliomas was significantly larger than that in

grade 2 astrocytomas, and similar to those in grade 3 and 4 astrocytomas. The ¹¹C-methionine uptake ratio was positively correlated to the microvessel area in grade 2 oligodendrogliomas. These findings are supported by recent evidence showing that the tumor relative cerebral blood volume (rCBV) is significantly higher in grade 2 oligodendrogliomas than in grade 2 astrocytomas [39]. Other reports have suggested that, the rCBV ratios correlate significantly with the histologic vascularity in gliomas [40, 41]. Our results indicate that an increase in the tumor vascular bed (i.e., an increased vessel surface area) could cause higher amino acid transportation followed by higher methionine uptake on PET in grade 2 oligodendrogliomas.

Our data from this study support the use of ¹¹C methionine PET as a marker of proliferative potential in the clinical management of astrocytomas. There is uncertainty, however, in how to interpret the variation of the ¹¹C methionine PET among oligodendrogliomas. We should note that malignant oligodendroglioma was not included in our analyses. It thus remains uncertain how ¹¹C-methionine uptake, tumor proliferative potential, and microvessel area correlate in the full series of oligodendrogliomas, including malignant subtypes. The negative correlation between cell proliferative potential and microvessel area among oligodendroglioma (presented in Fig. 5c) may have something to do with earlier evidence from Miwa et al. suggesting that ¹¹C-methionine uptake is decreased in the malignant component of oligodendroglial tumor [42]. On this point, however, we need further validation through an accumulation of more oligodendroglioma cases including anaplastic oligodendroglioma and oligoastrocytoma cases in future studies.

Conclusions

The ¹¹C-methionine uptake ratio in PET study was positively correlated with the proliferative index in astrocytomas. The methionine uptake was significantly greater in grade 2 oligodendrogliomas than in grade 2 astrocytomas, while the proliferative index was almost the same. The increase in tumor microvessel area without an accompanying increase in the microvessel count corresponded to the higher methionine uptake in grade 2 oligodendrogliomas. The determinant of the elevated uptake of methionine may differ between astrocytomas and oligodendrogliomas. An understanding of this issue is highly important in using ¹¹C-methionine imaging for the clinical management of gliomas.

Open Access This article is distributed under the terms of the Creative Commons Attribution Noncommercial License which permits any noncommercial use, distribution, and reproduction in any medium, provided the original author(s) and source are credited.

References

- Brant-Zawadzki M, Berry I, Osaki L et al (1986) Gd-DTPA in clinical MR of the brain: 1. Intraaxial lesions. *AJR Am J Roentgenol* 147:1223–1230
- Burger PC, Dubois PJ, Schold SC Jr et al (1983) Computerized tomographic and pathologic studies of the untreated, quiescent, and recurrent glioblastoma multiforme. *J Neurosurg* 58:159–169
- Burger PC, Heinz ER, Shibata T et al (1988) Topographic anatomy and CT correlations in the untreated glioblastoma multiforme. *J Neurosurg* 68:698–704
- Earnest Ft, Kelly PJ, Scheithauer BW et al (1988) Cerebral astrocytomas: histopathologic correlation of MR and CT contrast enhancement with stereotactic biopsy. *Radiology* 166:823–827
- Kelly PJ, Daumas-Duport C, Scheithauer BW et al (1987) Stereotactic histologic correlations of computed tomography- and magnetic resonance imaging-defined abnormalities in patients with glial neoplasms. *Mayo Clin Proc* 62:450–459
- Nariai T, Tanaka Y, Wakimoto H et al (2005) Usefulness of L-[methyl-¹¹C] methionine-positron emission tomography as a biological monitoring tool in the treatment of glioma. *J Neurosurg* 103:498–507
- Ogawa T, Inugami A, Hatazawa J et al (1996) Clinical positron emission tomography for brain tumors: comparison of fludeoxyglucose F 18 and L-methyl-¹¹C-methionine. *AJNR Am J Neuroradiol* 17:345–353
- Ogawa T, Shishido F, Kanno I et al (1993) Cerebral glioma: evaluation with methionine PET. *Radiology* 186:45–53
- Tovi M, Lilja A, Bergstrom M et al (1990) Delineation of gliomas with magnetic resonance imaging using Gd-DTPA in comparison with computed tomography and positron emission tomography. *Acta Radiol* 31:417–429
- Oldendorf WH, Szabo J (1976) Amino acid assignment to one of three blood–brain barrier amino acid carriers. *Am J Physiol* 230:94–98
- Sanchez del Pino MM, Peterson DR, Hawkins RA (1995) Neutral amino acid transport characterization of isolated luminal and abluminal membranes of the blood–brain barrier. *J Biol Chem* 270:14913–14918. doi:10.1074/jbc.270.48.28946
- Miwa K, Shinoda J, Yano H et al (2004) Discrepancy between lesion distributions on methionine PET and MR images in patients with glioblastoma multiforme: insight from a PET and MR fusion image study. *J Neurol Neurosurg Psychiatry* 75:1457–1462. doi:10.1136/jnnp.2003.028480
- Nariai T, Senda M, Ishii K et al (1997) Three-dimensional imaging of cortical structure, function and glioma for tumor resection. *J Nucl Med* 38:1563–1568
- Giammarile F, Cinotti LE, Jouvét A et al (2004) High and low grade oligodendrogliomas (ODG): correlation of amino-acid and glucose uptakes using PET and histological classifications. *J Neurooncol* 68:263–274. doi:10.1023/B:NEON.0000033384.43417.82
- Ribom D, Eriksson A, Hartman M et al (2001) Positron emission tomography (¹¹C)-methionine and survival in patients with low-grade gliomas. *Cancer* 92:1541–1549. doi:10.1002/1097-0142(20010915)92:6<1541::AID-CNCR1480>3.0.CO;2-D
- Ishiwata K, Kubota K, Murakami M et al (1993) Re-evaluation of amino acid PET studies: can the protein synthesis rates in brain and tumor tissues be measured in vivo? *J Nucl Med* 34:1936–1943
- Chung JK, Kim YK, Kim SK et al (2002) Usefulness of ¹¹C-methionine PET in the evaluation of brain lesions that are hypo- or isometabolic on ¹⁸F-FDG PET. *Eur J Nucl Med Mol Imaging* 29:176–182. doi:10.1007/s00259-001-0690-4
- Kim S, Chung JK, Im SH et al (2005) ¹¹C-methionine PET as a prognostic marker in patients with glioma: comparison with ¹⁸F-FDG PET. *Eur J Nucl Med Mol Imaging* 32:52–59. doi:10.1007/s00259-004-1598-6
- Kracht LW, Friese M, Herholz K et al (2003) Methyl-[¹¹C]-L-methionine uptake as measured by positron emission tomography correlates to microvessel density in patients with glioma. *Eur J Nucl Med Mol Imaging* 30:868–873
- Ardekani BA, Braun M, Hutton BF et al (1995) A fully automatic multimodality image registration algorithm. *J Comput Assist Tomogr* 19:615–623. doi:10.1097/00004728-199507000-00022
- Nagashima G, Aoyagi M, Wakimoto H et al (1995) Immunohistochemical detection of progesterone receptors and the correlation with Ki-67 labeling indices in paraffin-embedded sections of meningiomas. *Neurosurgery* 37:478–482. doi:10.1097/00006123-199509000-00016 (Discussion 483)
- Shin RW, Iwaki T, Kitamoto T et al (1991) Hydrated autoclave pretreatment enhances tau immunoreactivity in formalin-fixed normal and Alzheimer's disease brain tissues. *Lab Invest* 64:693–702
- Sato N, Suzuki M, Kuwata N et al (1999) Evaluation of the malignancy of glioma using ¹¹C-methionine positron emission tomography and proliferating cell nuclear antigen staining. *Neurosurg Rev* 22:210–214. doi:10.1007/s101430050018
- Langen KJ, Muhlensiepen H, Holschbach M et al (2000) Transport mechanisms of 3-[¹²³I]iodo-alpha-methyl-L-tyrosine in a human glioma cell line: comparison with [³H]methyl]-L-methionine. *J Nucl Med* 41:1250–1255
- Derlon JM, Chapon F, Noel MH et al (2000) Non-invasive grading of oligodendrogliomas: correlation between in vivo metabolic pattern and histopathology. *Eur J Nucl Med* 27:778–787. doi:10.1007/s002590000260
- Leon SP, Folkerth RD, Black PM (1996) Microvessel density is a prognostic indicator for patients with astroglial brain tumors. *Cancer* 77:362–372. doi:10.1002/(SICI)1097-0142(19960115)77:2<362::AID-CNCR20>3.0.CO;2-Z
- Vaquero J, Zurita M, Coca S et al (2000) Prognostic significance of clinical and angiogenesis-related factors in low-grade oligodendrogliomas. *Surg Neurol* 54:229–234. doi:10.1016/S0090-3019(00)00303-7 (Discussion 234)
- Oxender DL, Christensen HN (1963) Distinct mediating systems for the transport of neutral amino acids by the Ehrlich cell. *J Biol Chem* 238:3686–3699
- Broer S, Broer A, Hamprecht B (1997) Expression of the surface antigen 4F2hc affects system-L-like neutral-amino-acid-transport activity in mammalian cells. *Biochem J* 324(Pt 2): 535–541
- Bergstrom M, Lundqvist H, Ericson K et al (1987) Comparison of the accumulation kinetics of L-(methyl-¹¹C)-methionine and D-(methyl-¹¹C)-methionine in brain tumors studied with positron tomography. *Acta Radiol* 28:225–229
- Wienhard K, Herholz K, Coenen HH et al (1991) Increased amino acid transport into brain tumors measured by PET of L-(2-¹⁸F)fluorotyrosine. *J Nucl Med* 32:1338–1346
- Smith QR, Momma S, Aoyagi M et al (1987) Kinetics of neutral amino acid transport across the blood–brain barrier. *J Neurochem* 49:1651–1658. doi:10.1111/j.1471-4159.1987.tb01039.x
- Smith QR, Takasato Y (1986) Kinetics of amino acid transport at the blood–brain barrier studied using an in situ brain perfusion technique. *Ann N Y Acad Sci* 481:186–201. doi:10.1111/j.1749-6632.1986.tb27150.x
- Mosskin M, von Holst H, Bergstrom M, Collins VP, Eriksson L, Johnstrom P, Noren G (1987) Positron emission tomography with ¹¹C-methionine and computed tomography of intracranial tumours compared with histopathologic examination of multiple biopsies. *Acta Radiol* 28:673–681

35. Tynninen O, Aronen HJ, Ruhala M et al (1999) MRI enhancement and microvascular density in gliomas. Correlation with tumor cell proliferation. *Invest Radiol* 34:427–434. doi: [10.1097/00004424-199906000-00007](https://doi.org/10.1097/00004424-199906000-00007)
36. Kracht LW, Miletic H, Busch S et al (2004) Delineation of brain tumor extent with [¹¹C]L-methionine positron emission tomography: local comparison with stereotactic histopathology. *Clin Cancer Res* 10:7163–7170. doi: [10.1158/1078-0432.CCR-04-0262](https://doi.org/10.1158/1078-0432.CCR-04-0262)
37. Assimakopoulou M, Sotiropoulou-Bonikou G, Maraziotis T et al (1997) Microvessel density in brain tumors. *Anticancer Res* 17:4747–4753
38. Morimoto T, Aoyagi M, Tamaki M et al (2002) Increased levels of tissue endostatin in human malignant gliomas. *Clin Cancer Res* 8:2933–2938
39. Cha S, Tihan T, Crawford F et al (2005) Differentiation of low-grade oligodendrogliomas from low-grade astrocytomas by using quantitative blood-volume measurements derived from dynamic susceptibility contrast-enhanced MR imaging. *AJNR Am J Neuroradiol* 26:266–273
40. Aronen HJ, Gazit IE, Louis DN et al (1994) Cerebral blood volume maps of gliomas: comparison with tumor grade and histologic findings. *Radiology* 191:41–51
41. Sugahara T, Korogi Y, Kochi M et al (1998) Correlation of MR imaging-determined cerebral blood volume maps with histologic and angiographic determination of vascularity of gliomas. *AJR Am J Roentgenol* 171:1479–1486
42. Miwa K, Shinoda J, Yano H et al (2007) Relatively decreased ¹¹C-methionine uptake within the anaplastic component of a mixed-grade oligodendroglioma. *AJNR Am J Neuroradiol* 28:2005–2007. doi: [10.3174/ajnr.A0695](https://doi.org/10.3174/ajnr.A0695)